ELSEVIER

Comput. Methods Appl. Mech. Engrg. 190 (2001) 1937–1953

Computer methods in applied mechanics and engineering

www.elsevier.com/locate/cma

The analysis of an ill-posed problem using multi-scale resolution and second-order adjoint techniques

A.K. Alekseev [a], I. Michael Navon [b,*]

[a] *Department of Aerodynamics and Heat Transfer, RSC, ENERGIA, Korolev (Kaliningrad), Moscow Region 141070, Russian Federation*

[b] *Department of Mathematics and C.S.I.T., Florida State University, Tallahassee, FL 32306–4130, USA*

Received 7 October 1999

Abstract

A wavelet regularization approach is presented for dealing with an ill-posed problem of adjoint parameter estimation applied to estimating inflow parameters from down-flow data in an inverse convection case applied to the two-dimensional parabolized Navier–Stokes equations. The wavelet method provides a decomposition into two subspaces, by identifying both a well-posed as well as an ill-posed subspace, the scale of which is determined by finding the minimal eigenvalues of the Hessian of a cost functional measuring the lack of fit between model prediction and observed parameters. The control space is transformed into a wavelet space. The Hessian of the cost is obtained either by a discrete differentiation of the gradients of the cost derived from the first-order adjoint or by using the full second-order adjoint. The minimum eigenvalues of the Hessian are obtained either by employing a shifted iteration method [X. Zou, I.M. Navon, F.X. Le Dimet., Tellus 44A (4) (1992) 273] or by using the Rayleigh quotient. The numerical results obtained show the usefulness and applicability of this algorithm if the Hessian minimal eigenvalue is greater or equal to the square of the data error dispersion, in which case the problem can be considered as well-posed (i.e., regularized). If the regularization fails, i.e., the minimal Hessian eigenvalue is less than the square of the data error dispersion of the problem, the following wavelet scale should be neglected, followed by another algorithm iteration. The use of wavelets also allowed computational efficiency due to reduction of the control dimension obtained by neglecting the small-scale wavelet coefficients.

Keywords: Second-order adjoint problem; Ill-posed problem; Regularization; Wavelets and adjoint parameter estimation

1. Introduction

The method of well-posed subspace determination using multi-scale (wavelet) approach was proposed in [1] for the solution of ill-posed problems. This algorithm is significantly faster than the method of optimal decomposition of control space into "well-posed" and "ill-posed" subspaces based on the total set of eigenvalues. Nevertheless, the approach proposed in [1] is based on the direct search of eigenvalues and eigenvectors of an explicitly defined linear operator (more precisely, the product of forward and adjoint operators A^*A). As an alternative, we consider applying here an algorithm for finding the minimum eigenvalue of the Hessian of the cost functional based on the second-order adjoint approach presented in [2] to a nonlinear problem in the form of a system of coupled partial differential equations (PDEs).

The present paper describes an algorithm for determining a well-posed subspace using elements of both approaches presented in [1,2].

* Corresponding author. Tel.: +1-850-644-6560; fax: +1-850-644-0098.
E-mail address: navon@csit.fsu.edu (I. Michael Navon).

0045-7825/01/$ - see front matter
PII: S0045-7825(00)00299-1

Liu [11] gave a quantitative relation between the sensitivity of the mapping from the parameter space into the observation space. In this way, the Haar basis decomposes parameters to be estimated into parts with different sensitivity order, thus providing an easy method to identify suitability of multi-resolution methods for inverse problems.

The choice of the scale of wavelet transformation is determined by performing a subsequent search for the minimum eigenvalues of a Hessian obtained by considering the first- and second-order adjoint problems. The algorithm is based on cheap calculation of Hessian action using adjoint problems and on the information on the data error (we assume the data error dispersion σ to be known). We calculate the minimal eigenvalue of the Hessian of the cost functional using iterations and adjoint approach. If it is greater or equal to σ^2 then the problem is considered to be well-posed. If it is less than σ^2 then the following operations should be performed:

- Control space is transformed into wavelet space.
- The detailed coefficients of smallest scale are neglected (i.e. we are effectively decreasing the control space dimension by a factor of 2).
- Recalculate the Hessian minimal eigenvalue. If it is greater or equal to σ^2 then the problem is considered to be well-posed in this subspace and iterations are stopped. If it is less than σ^2 then the following scale should be neglected and the iteration is to be repeated.

This algorithm is implemented for a parabolized Navier–Stokes equations model. This model is used because these equations may be solved by marching along the X-coordinate, which provides for very fast computations. Despite its simplicity, this model correctly describes realistic and practically important flows with the restriction such that the flow is supersonic in the X-direction and viscous effects along this direction are negligible. The simplest example is the spreading of the propulsion jet in a supersonic airflow. The sketch of the flow-field and boundaries is presented in Fig. 1. The present state of experimental art provides abundant data on spatial distributions of velocity components, temperature, density, and concentrations in flow-field. These methods provide both high spatial resolution and high accuracy. Nevertheless, the direct measurement of flow parameters in regions of interest may prove to be difficult, for example, due to lack of access. The measurements may be located in some another zones. On the other hand, the estimation of total flow-field from measurement in some section may be of interest also. Both these problems may be reduced to the estimation of entrance boundary parameters from measurements in a downstream flow-field section (or set of sections). This problem may be posed in a variational statement, where the discrepancy between measured and calculated flow parameters is minimized. These problems are ill-posed and exhibit high instability in presence of data error [8]. The instability is much more serious for these problems due to their high nonlinearity and the solution failure at negative density or temperature. The parabolized Navier–Stokes equations are used herein as a realistic example of viscous flow, which may be solved in a very fast and computationally efficient way.

The present paper is organized as follows. In Section 2, we present the multi-scale regularization approach for the ill-posed problem of adjoint parameter estimation, based on the work of Liu et al. [1] along with use of the Fisher informational matrix for estimating the degree of the problem ill-posedness, based on the work of Alifanov et al. [4].

Section 3 consists of brief conclusions and a succinct presentation of the multi-scale regularization algorithm employed.

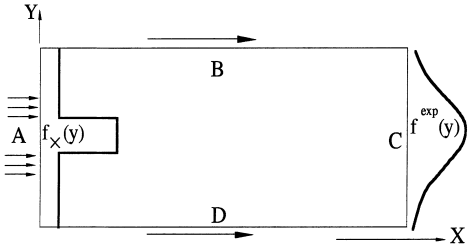

Fig. 1. Flow sketch. A – entrance boundary, C – section of measurements (outflow boundary).

Section 4 consists of a short presentation of first- and second-order adjoint methods for inverse-convection problems, followed in Section 5 by the presentation of the first- and second-order adjoint of the parabolized Navier–Stokes equations as well as the explicit formulation of the cost functional to be minimized for optimal parameter estimation.

Section 6 provides a brief presentation of the Lagrangian as a first step in the derivation of full expressions for the first- and second-order adjoint model.

Section 7 describes in detail the tangent linear and Lagrangian variation as a function of the control parameters for the parabolized Navier–Stokes equations. The technical details related to the adjoint problem statement are presented in Appendix A.

Section 8 presents the first-order adjoint model equations followed in Section 9 by the derivation of the second-order adjoint. Having in place the forward, tangent linear, first- and second-order adjoint models we proceed to calculate the spectrum bounds of the Hessian of the cost functional with respect to the control variables. This is done in Section 10 using a Rayleigh quotient and a calculation of the minimal eigenvalues by a shifted iteration method. Results of the optimal parameter estimation using the wavelet regularization procedure with different scales of wavelet transformation are presented for increasing Reynolds numbers and using different scales of regularization related to the wavelet transformation.

The parameters were initially perturbed with a random value in order to simulate the data error. Numerical tests show that the new algorithm performs successfully both in estimating and regularizing inflow parameters related to the inverse-convection problem described by the parabolized Navier–Stokes equations and that the Hessian minimal eigenvalue increases with increasing Reynolds numbers as well as with the increase in the wavelet scale.

Section 11 provides a comparison of the new method with the zeroth- and second-order Tikhonov regularization. The details of the first-order adjoint calculation are presented in Appendix A.

2. Multi-scale regularization

Algorithms for ill-posed problems may be often reduced to the solution of an ill-conditioned system of linear equations. The ill-conditioned operator may be represented in diagonal form using singular value decomposition. Some eigenvalues of this operator may be zero or very close to zero. The solution may then be searched in the subspace of those eigenvectors whose eigenvalues are greater than some value [3]. This method may be viewed as a variant of Occam's regularization where the "simplest" solution is defined as one composed of a minimum number of eigenvectors with large eigenvalues.

Let A be an operator (matrix) and ε be certain small value (to be considered below as the data mismatch $\varepsilon(v) = \|Av - b\|_H^2$).

We define boundary functions for subspace $U \subset V$ (V-being the control functions' space):

$$B_{\inf}(U) = \inf \frac{\|AX\|}{\|X\|}, \quad B_{\sup}(U) = \sup \frac{\|AX\|}{\|X\|}.$$

Using singular value decomposition, we can define the control functions' space V as a sum $V = V_\varepsilon^+ + V_\varepsilon^-$ of two subspaces, such that $B_{\inf}(V_\varepsilon^+) > \varepsilon$, $B_{\sup}(V_\varepsilon^-) < \varepsilon$. V_ε^+, is spanned by eigenvectors $\{v_1, v_2, \ldots, v_L\}$ while V_ε^- by $\{v_{L+1}, v_{L+2}, \ldots, v_N\}$. Herein, the eigenvectors are ordered according to the eigenvalues of magnitudes $\lambda_L > \varepsilon > \lambda_{L+1}$. We may neglect V_ε^- and search the solution only in V_ε^+ [1,3] for numerical stability. This approach implies the calculation of all eigenvalues and eigenvectors, which is a computationally intensive task.

Singular value decomposition may be replaced by a multi-scale (wavelet) decomposition [1]. We may construct a sequence of subspaces with decreasing $B_{\inf}$. This allows us to find two (suboptimal) subspaces $U_\varepsilon^-, U_\varepsilon^+ : B_{\inf}(U_\varepsilon^+) > \varepsilon$.

Multi-scale resolution is based on the sequence of subspaces: (V_j is a subspace spanned over the wavelet mother function of scale j)

$$V_0 \subset V_1 \subset V_2 \cdots \subset V_j \subset V.$$

The subspace of scale j may be defined also using W_j, which is a subspace spanned over the wavelet of scale j:

$$V_j = V_0 \oplus W_0 \oplus W_1 \oplus \cdots \oplus W_{j-1}.$$

The control functions' space may be written in the form

$$V = V_0 \oplus W_0 \oplus W_1 \oplus \cdots \oplus W_j \oplus \cdots$$

The space V may be decomposed into two subspaces for every scale j:

$$V = V_j + V_j^{\perp},$$

where $V_j^{\perp} = W_j + W_{j+1} + \cdots$ is the subspace of wavelets of high scale (details).

Work by Liu et al. [1] demonstrates (for Haar basis) that $B_{\sup}(V_j^{\perp}) \leqslant C \cdot 2^{-j/2}$, and for every ε we can find a j such that $B_{\sup}(V_j^{\perp}) \leqslant \varepsilon$. Thus, wavelet transformation provides an ordering of subspaces $V_j^{\perp}$ according to the scale j and the minimal eigenvalues. There is no similar proof for $B_{\inf}(V_j)$ (although such ordering seems to be quite natural). So, our numerical tests are performed for estimating $\lambda_{\min}$ for the sequence V_j depending on the scale j. According to Liu et al. [1], the discrete wavelet transformation is used for the approximation of the control functions

$$f(y) = a_0\varphi_0(y) + \sum_{j=0}^{J}\sum_{k=0}^{2^j-1} a_k^j W(2^j y - k),$$

which may be written in finite-dimensional form as

$$f_i = W \cdot a_k^j \quad (i = 1, \ldots, N),$$

where j is the scale, k translation, and N is the number of controls. The Daubechies-20 [5] transform (implemented via the pyramidal algorithm) was used, as it is more suitable for smooth functions in comparison with the Haar transformation. Numerical tests confirmed a decrease of $\lambda_{\min}(V_j)$ depending on the scale j.

The work in [1] concerns only linear problems. The minimization of $\varepsilon(v) = \|Av - b\|_H^2$ may be reduced to the solution of Euler equations $A^*Ax = A^*b$ and the subspaces of A^*A are studied. For nonlinear problems, the Hessian is used instead of the A^*A operator. An approach using the Fisher information matrix (approximating the Hessian in vicinity of the solution) is described in [4] for the estimation of problem ill-posedness.

Given the discrepancy (cost functional) $\varepsilon(u) = \sum_i (f_i^{\text{obs}} - f_i(u))^2$, where u is the vector of control parameters, the Hessian of the cost functional with respect to control parameters assumes the form

$$H_{jk} = \frac{\partial^2 \varepsilon}{\partial u_{jk}^2} = \sum_i \frac{\partial f_i}{\partial u_j}\frac{\partial f_i}{\partial u_k} - 2\sum_i \left(f_i^{\text{obs}} - f_i\right)\frac{\partial^2 f_i}{\partial u_j\,\partial u_k}.$$

Let $S_{ij} = \partial f_i/\partial u_j$ denote the sensitivity matrix (rectangular) and $M_{ij} = (\partial f_k/\partial u_i)(\partial f_k/\partial u_j)$ the informational matrix (square). When divided by data error dispersion, the Fisher matrix is defined by

$$M_{ij} = \sum_k \frac{1}{\sigma_k^2}\frac{\partial f_k}{\partial u_i}\frac{\partial f_k}{\partial u_j}.$$

The inverse matrix $D = M^{-1}$ is a dispersion matrix of the control parameters' error u_j. The magnitude of the Fisher informational matrix minimal eigenvalue compared with the data error $\lambda_{\min} \approx \sigma^2$ may be used for estimating the problem ill-posedness [4]. The calculation of the informational matrix is based on the system of sensitivity equations, which is more time and memory consuming compared with the adjoint approach.

3. The sequent multi-scale regularization algorithm

The use of adjoint methods provides a cheap way for the calculation of the Hessian action and, consequently, the bounds of its spectrum. Thus, we may not search for total spectrum of Hessian as it is done in [1]. We may consequently check subspaces from the viewpoint of minimum eigenvalue of the Hessian and the a priori known data error.

The schematic algorithm consists of the following stages:

1. We calculate the minimal eigenvalue of the Hessian of the cost functional. If it is greater or equal to σ^2 (σ-data error dispersion) then the problem is considered to be well-posed. If it is less than σ^2 the following operations should be performed:
2. Control space is transformed into wavelet space.
3. The detailed coefficients of the smallest scale are neglected (i.e., we are effectively decreasing the control space dimension by a factor of 2).
4. Recalculate the Hessian minimal eigenvalue. If it is greater or equal to σ^2 then the problem is considered to be well-posed in this subspace. If it is less than σ^2 then the following scale should be neglected and the iteration is to be repeated.

This algorithm is based on fast calculation of Hessian action that is connected with following adjoint problems.

4. Adjoint problems of the first- and second-order

The solution of the adjoint problem used for gradient calculation is the standard approach used for the inverse-convection problems [2,6]. The action of Hessian may be calculated by using the second-order adjoint approach [2]. In accordance with [2], we consider here the general scheme for second-order adjoint problem. Herein X denotes the marching coordinate (the time analogue), f is a vector of variables (flow parameters), C is a matrix of observation, ε is the discrepancy between model calculation and the observations, and U is a vector of the control variables (parameters on the inflow boundary).

Forward problem:

$$\frac{\mathrm{d}f}{\mathrm{d}X} = F(f), \quad f(0) = U, \quad \varepsilon(U) = \frac{1}{2}\int_0^Y \|Cf - f_{\mathrm{obs}}\|^2 \,\mathrm{d}Y. \tag{1}$$

First-order adjoint problem:

$$\frac{\mathrm{d}\Psi}{\mathrm{d}X} + \frac{\partial F^{\mathrm{T}}}{\partial f}\,\Psi = C^{\mathrm{T}}(Cf - f_{\mathrm{obs}}), \quad \Psi(1) = 0, \quad \nabla\varepsilon(U) = -\Psi(0). \tag{2}$$

Tangent problem:

$$\frac{\mathrm{d}\hat{f}}{\mathrm{d}X} = \frac{\partial F}{\partial f}\hat{f}, \quad \hat{f}(0) = u. \tag{3}$$

Second-order adjoint problem (tangent to first-order adjoint):

$$\frac{\mathrm{d}\hat{\Psi}}{\mathrm{d}X} + \left[\frac{\partial^2 F}{\partial f^2}\hat{f}\right]\Psi + \left[\frac{\partial F^{\mathrm{T}}}{\partial f}\right]\hat{\Psi} = C^{\mathrm{T}}C\hat{f}, \quad \hat{\Psi}(1) = 0, \quad \nabla\hat{\varepsilon}(U) = H(U)u = -\hat{\Psi}(0). \tag{4}$$

Thus, the Hessian action on vector U may be obtained by sequentially solving Eqs. (1)–(4) (all about the forward problem from computer resources viewpoint). We consequently solve the following four initial-boundary problems:

1. Forward problem, Eq. (1) (X is increasing).
2. First-order adjoint problem, Eq. (2) (X is decreasing, i.e., backward in time).
3. Tangent problem, Eq. (3) (X is increasing).
4. Second-order adjoint problem, Eq. (4) (X is decreasing).

In order to find the Hessian, the calculations for N operations should be performed, so the Hessian's computational cost equals $4N$.

Numerical differentiation using the Hessian-free finite difference expression (see Wang et al. [9])

$$H\,\mathrm{d}u = (\mathrm{grad}(u + a\,\mathrm{d}u) - \mathrm{grad}(u))/a$$

requires also four solutions of this type of problem but is somewhat less accurate.

In the following, we consider the scheme (1)–(4) for the two-dimensional parabolized Navier–Stokes equations.

5. First- and second-order adjoint problems for parabolized Navier–Stokes equations

We consider here the problem estimation of the inflow parameters $u = f_\infty(Y) = (\rho(Y), U(Y), V(Y), T(Y))$ from outflow measurements (Fig. 1). The flow is two-dimensional supersonic laminar one governed by the parabolized Navier–Stokes equations (viscosity is neglected in the X-direction, which rapidly decreases the computational time, but at a sacrifice of the applicability range).

$$\frac{\partial(\rho U)}{\partial X} + \frac{\partial(\rho V)}{\partial Y} = 0, \tag{5}$$

$$U\frac{\partial U}{\partial X} + V\frac{\partial U}{\partial Y} + \frac{1}{\rho}\frac{\partial P}{\partial X} = \frac{1}{Re\,\rho}\frac{\partial^2 U}{\partial Y^2}, \tag{6}$$

$$U\frac{\partial V}{\partial X} + V\frac{\partial V}{\partial Y} + \frac{1}{\rho}\frac{\partial P}{\partial Y} = \frac{4}{3\rho Re}\frac{\partial^2 V}{\partial Y^2}, \tag{7}$$

$$U\frac{\partial e}{\partial X} + V\frac{\partial e}{\partial Y} + (\kappa - 1)e\left(\frac{\partial U}{\partial X} + \frac{\partial V}{\partial Y}\right) = \frac{1}{\rho}\left(\frac{\kappa}{Re\,Pr}\frac{\partial^2 e}{\partial Y^2} + \frac{4}{3Re}\left(\frac{\partial U}{\partial Y}\right)^2\right), \tag{8}$$

$$e = C_v T = R/(\kappa - 1)T, \quad P = (\kappa - 1)\rho e, \quad (X, Y) \in Q = (0 < X < 1,\ 0 < Y < 1).$$

The boundary conditions of the undisturbed external flow (9) are used on the boundaries $Y = 0,\ Y = 1$.

$$\varepsilon(f_\infty(Y)) = \int\int_Y (f_{\mathrm{obs}}(X, Y) - f(X, Y))^2 \delta(X - X_m)\delta(Y - Y_m)\,\mathrm{d}X\,\mathrm{d}Y. \tag{9}$$

We search for $f_\infty(Y) = (\rho(Y), U(Y), V(Y), e(Y))$ using outflow data (Fig. 1) by minimizing discrepancy cost functional

$$\varepsilon(f_\infty(Y)) = \int\int_Y (f_{\mathrm{obs}}(X, Y) - f(X, Y))^2 \delta(X - X_m)\delta(Y - Y_m)\,\mathrm{d}X\,\mathrm{d}Y. \tag{10}$$

6. Lagrangian

According to [2,4,6], we define the Lagrangian using the weak form of Eqs. (5)–(8) and the discrepancy (10).

$$\begin{aligned}\varepsilon_0(f_\infty(Y)) = \varepsilon(f_\infty(Y)) &+ \int_X \int_Y \left(\frac{\partial(\rho U)}{\partial X} + \frac{\partial(\rho V)}{\partial Y} \right) \Psi_\rho(X,Y)\, \mathrm{d}X\, \mathrm{d}Y \\ &+ \int_X \int_Y \left(U\frac{\partial U}{\partial X} + V\frac{\partial U}{\partial Y} + \frac{1}{\rho}\frac{\partial P}{\partial X} - \frac{1}{Re\,\rho}\frac{\partial^2 U}{\partial Y^2} \right) \Psi_U(X,Y)\, \mathrm{d}X\, \mathrm{d}Y \\ &+ \int_X \int_Y \left(U\frac{\partial V}{\partial X} + V\frac{\partial V}{\partial Y} + \frac{1}{\rho}\frac{\partial P}{\partial Y} - \frac{4}{3Re\,\rho}\frac{\partial^2 V}{\partial Y^2} \right) \Psi_V(X,Y)\, \mathrm{d}X\, \mathrm{d}Y \\ &+ \int_X \int_Y \left(U\frac{\partial e}{\partial X} + V\frac{\partial e}{\partial Y} + (\kappa-1)e\left(\frac{\partial U}{\partial X} + \frac{\partial V}{\partial Y} \right) - \frac{\kappa}{\rho Re\,Pr}\frac{\partial^2 e}{\partial Y^2} - \frac{4}{3Re\,\rho}\left(\frac{\partial U}{\partial Y} \right)^2 \right) \\ &\times\ \Psi_e(X,Y)\, \mathrm{d}X\, \mathrm{d}Y. \end{aligned} \tag{11}$$

We consider $(\Psi_\rho(X,Y), \Psi_U(X,Y), \Psi_V(X,Y), \Psi_e(X,Y)) \in H^{1,2}(Q)$, where $H^{1,2}(Q)$ is a Hilbert space of first- and second-order distributions.

7. Tangent linear problem and Lagrangian variation

The tangent linear problem should be stated for determination of the Lagrangian's (11) variation as a function of the control parameters' variation. We disturb the boundary condition (9)

$$\Delta f(0,Y) = \Delta f_\infty(Y) \tag{12}$$

and obtain corresponding variations of $\Delta\rho, \Delta U, \Delta V, \Delta e$ in (5)–(8) by subtracting the undisturbed variables.

$$U\frac{\partial(\Delta\rho)}{\partial X} + \rho\frac{\partial(\Delta U)}{\partial X} + \rho\frac{\partial(\Delta V)}{\partial Y} + V\frac{\partial(\Delta\rho)}{\partial Y} + \Delta\rho\frac{\partial U}{\partial X} + \Delta U\frac{\partial\rho}{\partial X} + \Delta\rho\frac{\partial V}{\partial Y} + \Delta V\frac{\partial\rho}{\partial Y} = 0, \tag{13}$$

$$\begin{aligned} &U\frac{\partial\Delta U}{\partial X} + \Delta U\frac{\partial U}{\partial X} + \Delta V\frac{\partial U}{\partial Y} + V\frac{\partial\Delta U}{\partial Y} - \frac{1}{\rho Re}\frac{\partial^2\Delta U}{\partial Y^2} + \frac{\Delta\rho}{\rho^2 Re}\frac{\partial^2 U}{\partial Y^2} - \frac{\Delta\rho}{\rho^2}\frac{\partial P}{\partial X} \\ &+ \frac{(\kappa-1)}{\rho}\left(\Delta\rho\frac{\partial e}{\partial X} + e\frac{\partial\Delta\rho}{\partial X} + \rho\frac{\partial\Delta e}{\partial X} + \Delta e\frac{\partial\rho}{\partial X} \right) = 0, \end{aligned} \tag{14}$$

$$\begin{aligned} &U\frac{\partial\Delta V}{\partial X} + \Delta U\frac{\partial V}{\partial X} + \Delta V\frac{\partial V}{\partial Y} + V\frac{\partial\Delta V}{\partial Y} - \frac{4}{3\rho\,Re}\frac{\partial^2\Delta V}{\partial Y^2} + \frac{4\Delta\rho}{3\rho^2\,Re}\frac{\partial^2 V}{\partial Y^2} - \frac{\Delta\rho}{\rho^2}\frac{\partial P}{\partial Y} \\ &+ \frac{(\kappa-1)}{\rho}\left(\Delta\rho\frac{\partial e}{\partial Y} + e\frac{\partial\Delta\rho}{\partial Y} + \rho\frac{\partial\Delta e}{\partial Y} + \Delta e\frac{\partial\rho}{\partial Y} \right) = 0, \end{aligned} \tag{15}$$

$$\begin{aligned} &U\frac{\partial\Delta e}{\partial X} + \Delta U\frac{\partial e}{\partial X} + \Delta V\frac{\partial e}{\partial Y} + V\frac{\partial\Delta e}{\partial Y} + (\kappa-1)\Delta e\left(\frac{\partial U}{\partial X} + \frac{\partial V}{\partial Y} \right) + (\kappa-1)e\left(\frac{\partial\Delta U}{\partial X} + \frac{\partial\Delta V}{\partial Y} \right) \\ &- \frac{1}{\rho}\left(\frac{\kappa}{Re\,Pr}\frac{\partial^2\Delta e}{\partial Y^2} - \frac{\kappa}{Re\,Pr}\frac{\Delta\rho}{\rho}\frac{\partial^2 e}{\partial Y^2} + \frac{8}{3Re}\left(\frac{\partial\Delta U}{\partial Y} \right)\left(\frac{\partial U}{\partial Y} \right) - \frac{\Delta\rho}{\rho}\frac{4}{3Re}\left(\frac{\partial U}{\partial Y} \right)^2 \right) = 0, \end{aligned} \tag{16}$$

$$\Delta f(0,Y) = \Delta f_\infty(Y), \quad \Delta f(X,1) = \Delta f_\infty(1), \quad \Delta f(X,0) = \Delta f_\infty(0). \tag{17}$$

The tangent linear problem is used not only for deriving the first-order adjoint problem but also serves as a component for solution of the second-order adjoint problem (Hessian action calculation).

8. First-order adjoint equations

We look for $(\Psi_\rho, \Psi_U, \Psi_V, \Psi_e)$ such that $\Delta\varepsilon_0 = \int_Y \mathrm{grad}(\varepsilon)\Delta f_\infty(Y)\,\mathrm{d}Y$ while all other first-order terms vanish. Details of first-order adjoint (FOA) derivation are presented in Appendix A.

$$
\begin{aligned}
&U\frac{\partial\Psi_\rho}{\partial X} + V\frac{\partial\Psi_\rho}{\partial Y} + (\kappa-1)\frac{\partial(\Psi_V e/\rho)}{\partial Y} + (\kappa-1)\frac{\partial(\Psi_U e/\rho)}{\partial X} - \frac{\kappa-1}{\rho}\left(\frac{\partial e}{\partial Y}\Psi_V + \frac{\partial e}{\partial X}\Psi_U\right)\\
&\quad + \left(\frac{1}{\rho^2}\frac{\partial P}{\partial X} - \frac{1}{\rho^2 Re}\frac{\partial^2 U}{\partial Y^2}\right)\Psi_U + \frac{1}{\rho^2}\left(\frac{\partial P}{\partial Y} - \frac{4}{3Re}\frac{\partial^2 V}{\partial Y^2}\right)\Psi_V - \frac{1}{\rho^2}\left(\frac{\gamma}{Re\,Pr}\frac{\partial^2 e}{\partial Y^2} + \frac{4}{3Re}\left(\frac{\partial U}{\partial Y}\right)^2\right)\Psi_e\\
&\quad + 2(\rho_{\mathrm{obs}}(X,Y) - \rho(X,Y))\delta(X-X_m)\delta(Y-Y_m) = 0,
\end{aligned}
\tag{18}
$$

$$
\begin{aligned}
&U\frac{\partial\Psi_U}{\partial X} + \frac{\partial(\Psi_U V)}{\partial Y} + \rho\frac{\partial\Psi_\rho}{\partial X} - \left(\frac{\partial V}{\partial X}\Psi_V + \frac{\partial e}{\partial X}\Psi_e\right) + \frac{\partial}{\partial X}\left(\frac{P}{\rho}\Psi_e\right) + \frac{\partial^2}{\partial Y^2}\left(\frac{1}{\rho Re}\Psi_U\right)\\
&\quad - \frac{\partial}{\partial Y}\left(\frac{8}{3Re}\frac{\partial U}{\partial Y}\Psi_e\right) + 2(U_{\mathrm{obs}}(X,Y) - U(X,Y))\delta(X-X_m)\delta(Y-Y_m) = 0,
\end{aligned}
\tag{19}
$$

$$
\begin{aligned}
&\frac{\partial(U\Psi_V)}{\partial X} + V\frac{\partial\Psi_V}{\partial Y} - \left(\frac{\partial U}{\partial Y}\Psi_U + \frac{\partial e}{\partial Y}\Psi_e\right) + \rho\frac{\partial\Psi_\rho}{\partial Y} + \frac{\partial}{\partial Y}\left(\frac{P}{\rho}\Psi_e\right) + \frac{4}{3Re}\frac{\partial^2}{\partial Y^2}\left(\frac{\Psi_V}{\rho}\right)\\
&\quad + 2(V_{\mathrm{obs}}(X,Y) - V(X,Y))\delta(X-X_m)\delta(Y-Y_m) = 0,
\end{aligned}
\tag{20}
$$

$$
\begin{aligned}
&\frac{\partial(U\Psi_e)}{\partial X} + \frac{\partial(V\Psi_e)}{\partial Y} - \frac{\kappa-1}{\rho}\left(\frac{\partial\rho}{\partial Y}\Psi_V + \frac{\partial\rho}{\partial X}\Psi_U\right) - (\kappa-1)\left(\frac{\partial U}{\partial X} + \frac{\partial V}{\partial Y}\right)\Psi_e + (\kappa-1)\frac{\partial\Psi_V}{\partial Y}\\
&\quad + (\kappa-1)\frac{\partial\Psi_U}{\partial X} + \frac{\kappa}{Re\,Pr}\frac{\partial^2}{\partial Y^2}\left(\frac{\Psi_e}{\rho}\right) + 2(e_{\mathrm{obs}}(X,Y) - e(X,Y))\delta(X-X_m)\delta(Y-Y_m) = 0.
\end{aligned}
\tag{21}
$$

Initial $(X=1)$ and boundary $(Y=0,\ Y=1)$ conditions yield:

$$
\begin{aligned}
&(U\Psi_\rho + \Psi_U e/\rho)\big|^{x=1} = 0, && \Psi_\rho\big|^{Y=1} = 0, && \Psi_\rho\big|_{Y=0} = 0,\\
&(U\Psi_U + \Psi_\rho\rho + \Psi_e(\kappa-1)e)\big|^{x=1} = 0, && \Psi_U\big|^{Y=1} = 0, && \Psi_U\big|_{Y=0} = 0,\\
&(U\Psi_e + (\kappa-1)\Psi_U)\big|^{X=1} = 0, && \Psi_e\big|^{Y=1} = 0, && \Psi_e\big|_{Y=0} = 0,\\
&(\Psi_V)\big|^{x=1} = 0, && \Psi_V\big|^{Y=1} = 0, && \Psi_V\big|_{Y=0} = 0.
\end{aligned}
\tag{22}
$$

If Eqs. (18)–(22) are satisfied then

$$
\begin{aligned}
\Delta\varepsilon_0(f_\infty(Y)) = &\int_Y ((\Psi_e U + (\kappa-1)\Psi_U)\Delta e_\infty(Y))|_{X=0}\,\mathrm{d}Y + \int_Y \big((\Psi_\rho U + (\kappa-1)\Psi_U e/\rho)\Delta\rho_\infty(Y)\big)|_{X=0}\,\mathrm{d}Y\\
&+ \int_Y \big((\Psi_U U + \rho\Psi_\rho + (\kappa-1)\Psi_e e)\Delta U_\infty(Y)\big)|_{X=0}\,\mathrm{d}Y + \int_Y (\Psi_V U\Delta V_\infty(Y))|_{X=0}\,\mathrm{d}Y.
\end{aligned}
\tag{23}
$$

This expression provides the fast calculation of the discrepancy gradient using both flow and adjoint field parameters. It also serves as the basis for calculating the second-order information (action of Hessian).

9. Second-order adjoint problem

According to Eq. (4), we can pose the second-order adjoint problem for Q_ρ, Q_U, Q_V, Q_e:

$$
\begin{aligned}
&U\frac{\partial Q_\rho}{\partial X}+V\frac{\partial Q_\rho}{\partial Y}+(\kappa-1)\frac{\partial(Q_V e/\rho)}{\partial Y}+(\kappa-1)\frac{\partial(Q_U e/\rho)}{\partial X}-\frac{\kappa-1}{\rho}\left(\frac{\partial e}{\partial Y}Q_V+\frac{\partial e}{\partial X}Q_U\right)\\
&+\left(\frac{1}{\rho^2}\frac{\partial P}{\partial X}-\frac{1}{\rho^2 Re}\frac{\partial^2 U}{\partial Y^2}\right)Q_U+\frac{1}{\rho^2}\left(\frac{\partial P}{\partial Y}-\frac{4}{3Re}\frac{\partial^2 V}{\partial Y^2}\right)Q_V-\frac{1}{\rho^2}\left(\frac{\gamma}{Re\,Pr}\frac{\partial^2 e}{\partial Y^2}+\frac{4}{3Re}\left(\frac{\partial U}{\partial Y}\right)^2\right)Q_e\\
&\quad=2\Delta\rho\delta(X-X_m)\delta(Y-Y_m)-\Delta U\frac{\partial\Psi_\rho}{\partial X}-\Delta V\frac{\partial\Psi_\rho}{\partial Y}-(\kappa-1)\frac{\partial(\Psi_V\Delta(e/\rho))}{\partial Y}-(\kappa-1)\frac{\partial(\Psi_U\Delta(e/\rho))}{\partial X}\\
&\qquad+\frac{\kappa-1}{\rho}\left(\frac{\partial\Delta e}{\partial Y}\Psi_V+\frac{\partial\Delta e}{\partial X}\Psi_U\right)-\left(\frac{1}{\rho^2}\frac{\partial\Delta P}{\partial X}-\frac{1}{\rho^2 Re}\frac{\partial^2\Delta U}{\partial Y^2}\right)\Psi_U-\frac{1}{\rho^2}\left(\frac{\partial\Delta P}{\partial Y}-\frac{4}{3Re}\frac{\partial^2\Delta V}{\partial Y^2}\right)\Psi_V\\
&\qquad+\frac{1}{\rho^2}\left(\frac{\gamma}{Re\,Pr}\frac{\partial^2\Delta e}{\partial Y^2}+\frac{4}{3Re}\left(\frac{\partial\Delta U}{\partial Y}\right)^2\right)\Psi_e-\frac{\kappa-1}{\rho^2}\Delta\rho\left(\frac{\partial e}{\partial Y}\Psi_V+\frac{\partial e}{\partial X}\Psi_U\right)\\
&\qquad+\left(\frac{2}{\rho^3}\frac{\partial P}{\partial X}-\frac{1}{\rho^3 Re}\frac{\partial^2 U}{\partial Y^2}\right)\Delta\rho\Psi_U+\frac{2}{\rho^3}\left(\frac{\partial P}{\partial Y}-\frac{4}{3Re}\frac{\partial^2 V}{\partial Y^2}\right)\Delta\rho\Psi_V\\
&\qquad-\frac{2}{\rho^3}\left(\frac{\gamma}{Re\,Pr}\frac{\partial^2 e}{\partial Y^2}+\frac{4}{3Re}\left(\frac{\partial U}{\partial Y}\right)^2\right)\Delta\rho\Psi_e,
\end{aligned}
\tag{24}
$$

$$
\begin{aligned}
&U\frac{\partial Q_U}{\partial X}+\frac{\partial(Q_U V)}{\partial Y}+\rho\frac{\partial Q_\rho}{\partial X}-\left(\frac{\partial V}{\partial X}Q_V+\frac{\partial e}{\partial X}Q_e\right)+\frac{\partial}{\partial X}\left(\frac{P}{\rho}Q_e\right)+\frac{\partial^2}{\partial Y^2}\left(\frac{1}{\rho Re}Q_U\right)-\frac{\partial}{\partial Y}\left(\frac{8}{3Re}\frac{\partial U}{\partial Y}Q_e\right)\\
&\quad=+2\Delta U\delta(X-X_m)\delta(Y-Y_m)-\Delta U\frac{\partial\Psi_U}{\partial X}-\frac{\partial(\Psi_U\Delta V)}{\partial Y}+\Delta\rho\frac{\partial\Psi_\rho}{\partial X}-\left(\frac{\partial\Delta V}{\partial X}\Psi_V+\frac{\partial\Delta e}{\partial X}\Psi_e\right)\\
&\qquad+\frac{\partial}{\partial X}\left(\Delta\left(\frac{P}{\rho}\right)\Psi_e\right)+\frac{\partial^2}{\partial Y^2}\left(\frac{\Delta\rho}{\rho^2 Re}\Psi_U\right)+\frac{\partial}{\partial Y}\left(\frac{8}{3Re}\frac{\partial\Delta U}{\partial Y}\Psi_e\right),
\end{aligned}
\tag{25}
$$

$$
\begin{aligned}
&\frac{\partial(UQ_V)}{\partial X}+V\frac{\partial Q_V}{\partial Y}-\left(\frac{\partial U}{\partial Y}Q_U+\frac{\partial e}{\partial Y}Q_e\right)+\rho\frac{\partial Q_\rho}{\partial Y}+\frac{\partial}{\partial Y}\left(\frac{P}{\rho}Q_e\right)+\frac{4}{3Re}\frac{\partial^2}{\partial Y^2}\left(\frac{Q_V}{\rho}\right)\\
&\quad=+2\Delta V\delta(X-X_m)\delta(Y-Y_m)-\frac{\partial(\Delta U\Psi_V)}{\partial X}-\Delta V\frac{\partial\Psi_V}{\partial Y}+\left(\frac{\partial\Delta U}{\partial Y}\Psi_U+\frac{\partial\Delta e}{\partial Y}\Psi_e\right)\\
&\qquad-\Delta\rho\frac{\partial\Psi_\rho}{\partial Y}-\frac{\partial}{\partial Y}\left(\Delta\frac{P}{\rho}\Psi_e\right)+\frac{4}{3Re}\frac{\partial^2}{\partial Y^2}\left(\frac{\Psi_V\Delta\rho}{\rho^2}\right),
\end{aligned}
\tag{26}
$$

$$
\begin{aligned}
&\frac{\partial(UQ_e)}{\partial X}+\frac{\partial(VQ_e)}{\partial Y}-\frac{\kappa-1}{\rho}\left(\frac{\partial\rho}{\partial Y}Q_V+\frac{\partial\rho}{\partial X}Q_U\right)-(\kappa-1)\left(\frac{\partial U}{\partial X}+\frac{\partial V}{\partial Y}\right)Q_e+(\kappa-1)\frac{\partial Q_V}{\partial Y}\\
&\quad+(\kappa-1)\frac{\partial Q_U}{\partial X}+\frac{\kappa}{Re\,Pr}\frac{\partial^2}{\partial Y^2}\left(\frac{Q_e}{\rho}\right)\\
&\qquad=2\Delta e\delta(X-X_m)\delta(Y-Y_m)-\frac{\partial(\Delta U\Psi_e)}{\partial X}-\frac{\partial(\Delta V\Psi_e)}{\partial Y}+\frac{\kappa-1}{\rho}\left(\frac{\partial\Delta\rho}{\partial Y}\Psi_V+\frac{\partial\Delta\rho}{\partial X}\Psi_U\right)\\
&\qquad\quad+(\kappa-1)\left(\frac{\partial\Delta U}{\partial X}+\frac{\partial\Delta V}{\partial Y}\right)\Psi_e-\frac{\kappa-1}{\rho^2}\left(\frac{\partial\rho}{\partial Y}\Psi_V+\frac{\partial\rho}{\partial X}\Psi_U\right)\Delta\rho+\frac{\kappa\Delta\rho}{Re\,Pr}\frac{\partial^2}{\partial Y^2}\left(\frac{\Psi_e}{\rho^2}\right).
\end{aligned}
\tag{27}
$$

Initial data $D(X=1)$

$$Q^{x=1}=0.$$

Boundary conditions at B, C $(Y = 0, Y = 1) : \partial Q/\partial Y = 0$.

$$\text{Hessian action on } \Delta f_\infty : H(f_\infty)\Delta f_\infty = -Q(0). \tag{28}$$

This expression provides a fast and precise calculation of Hessian action on a vector, which is the basis for the considered algorithm.

10. Hessian spectrum bounds calculation

For obtaining the Hessian action calculation we should solve the forward, tangent linear, first-order adjoint, and second-order adjoint problems. This is a very difficult task to accomplish from the code debugging viewpoint, and the full correctness of the second-order adjoint problem was not fully verified so far. Instead, the Hessian action was calculated by using the Hessian-free differentiation gradients [10] obtained from the first-order adjoint problem in the form:

$$H\,\mathrm{d}u = (\mathrm{grad}(u + a\,\mathrm{d}u) - \mathrm{grad}(u))/a.$$

The codes for the forward (5)–(8) and first-order adjoint (21)–(24) problems were fully verified for correctness.

The flow-field was computed by marching along X from $X = 0$ to $X = 1$. The adjoint problem was solved by marching along the X-coordinate in the backward direction (from $X = 1$ to $X = 0$). The finite difference algorithm was used for the solution of both the forward and adjoint problems. The algorithm is second order accurate in Y-direction and of first-order accuracy in the X-direction. The forward and adjoint problems were solved using the same grid.

We used the limited memory Quasi-Newton LBFGS method of large-scale optimization [7] to perform the minimization.

The iterations $X_{m+1} = HX_m;\ \lambda = \max(X_{m+1})/\max(X_m)$ are used for the maximum eigenvalue calculation. The minimum eigenvalue is calculated by a method of shifted iteration [2] $(M * E - H)$, where M is the eigenvalues' majorant and E is the unit matrix.

The minimum eigenvalue is calculated also by using the Rayleigh quotient algorithm:

$$R(X) = \frac{(HX, X)}{(X, X)}, \quad \min(R(X)) = \lambda_{\min}, \quad \mathrm{grad}(R(X)) = C(HX - R(X)X).$$

Iterations were performed using the steepest descent method:

$$X^{k+1} = X^x - a(HX - R(X)X).$$

When minimal eigenvalues are relatively large (to 10^{-3}), both algorithms present similar results $(Re = 10^7, \lambda_{\min} = 3.1\text{–}3.7 \times 10^{-2})$. For smaller eigenvalues the Rayleigh quotient turned out to be more accurate.

We now consider the minimum eigenvalue from the viewpoint of ill-posed problems description. Numerical results (when Mach number equals 4, while the Reynolds numbers vary in the range 10^2–10^7) demonstrated that the $\lambda_{\min}$ is increasing as the Reynolds number increases. This is connected with the changes in dissipative loss of information. (Herein, large Reynolds numbers (10^7) are formal coefficients at viscous terms). Nevertheless, the qualitative variation of the eigenvalues is correlated with the physics of the process.

The quality of the solution is also correlated to $\lambda_{\min}$, (Fig. 2). The low Reynolds numbers (high viscosity) correlate with small eigenvalues in Table 1 and poor quality of corresponding curves in Fig. 2.

Calculations were performed for estimating the variation of the $\lambda_{\min}$ eigenvalue with the change of scale j. The discrete wavelet transformation was used for control functions approximation.

The Daubechies-20 transformation [5] was used. The magnitude of $\lambda_{\min}$ $(Re = 1000)$ for different scales is presented in Table 2.

The value of $\lambda_{\min}$ increases as the scale increases in accordance with results of [5]. If we chose scales j such that $\lambda_{\min} \approx \sigma^2$ (where σ is data error dispersion) then we obtain a well-posed subspace of control functions. The subspaces of smaller scales do not contain useful information and can cause the instability.

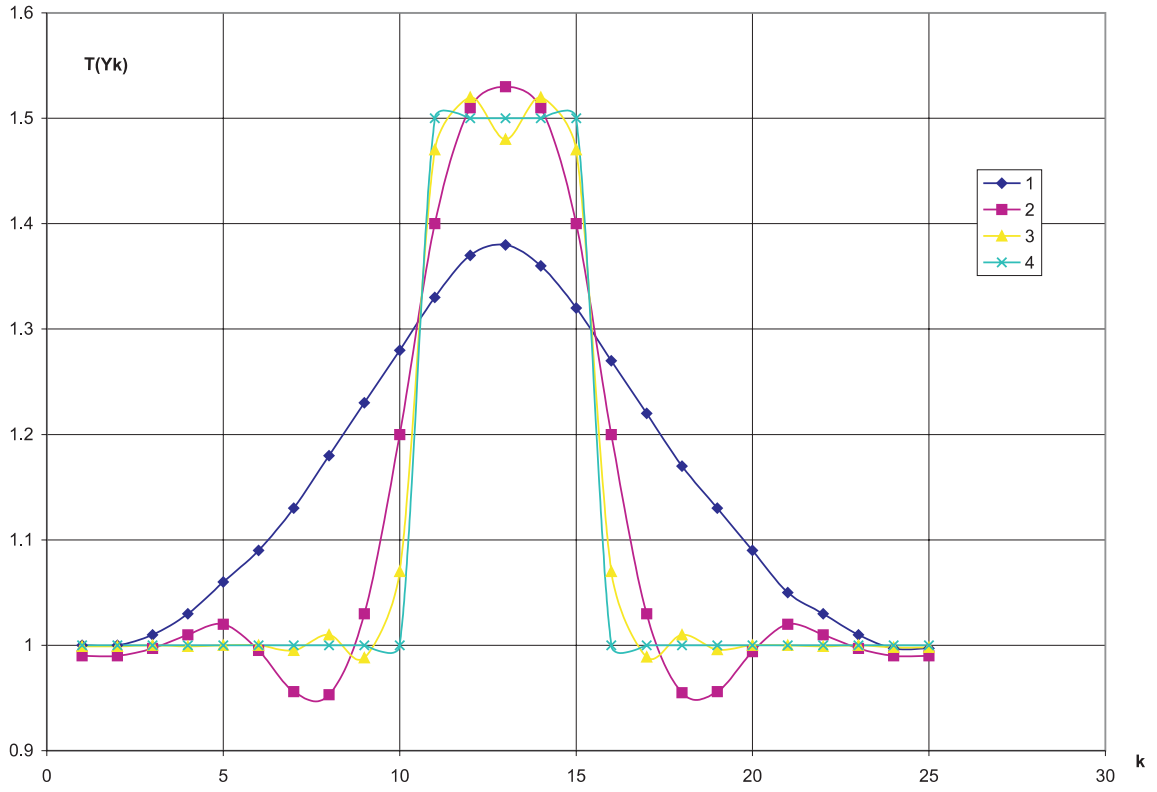

Fig. 2. The quality of the solution $(T(y))$ for different Re ($Re = 10^2, 10^3, 10^4, 10^7$ (10^7 coincides with exact)) numbers. It is correlated to $\lambda_{\min}$.

Table 1

Re	100	1000	10^4	10^7
$\lambda_{\min}$	8.6×10^{-6}	5.5×10^{-5}	6.4×10^{-3}	3.4×10^{-2}

Table 2

J	6	5	4	3
$\lambda_{\min}$	9×10^{-5}	1.5×10^{-4}	8.4×10^{-4}	9.9×10^{-3}

Fig. 3 presents results of all parameters (e, ρ, U, V) ($J = 6, N = 256$ parameters) estimation ($Re = 10\,000$) using different scales of wavelet transformation. Fig. 4 presents same results for e (temperature) only. The instability was developing from data error $\sigma = 0.01$. The use of 128 parameters ($J = 5$) (we neglected the detailed information of finest scale) cured the instability. The following subspaces presented similar results. The corresponding minimum eigenvalues are presented in Table 3. The success obtained is due to the smoothness of the searched control functions. If discontinuities are present, then large wavelet coefficients are present at every scale and the regularization negatively affects the approximation in a more significant way.

The wavelet transformation provides the parameters regularization using some physical properties of the control functions (their smallest scale, for example). It requires only about $\ln(N)$ calculation of eigenvalues instead of N when the entire Hessian spectrum is used.

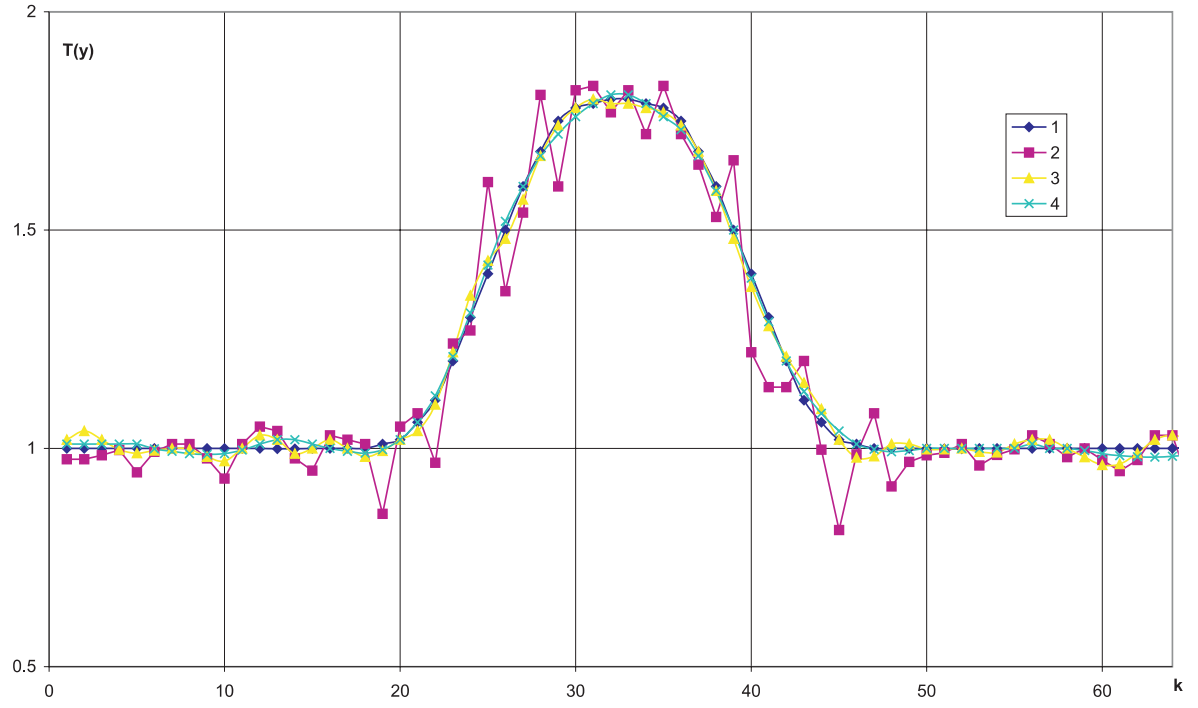

Fig. 3. Results of all parameters (e, ρ, U, V) estimation using different scales of wavelet transformation ($Re = 10\,000$): (1) exact inflow data ($J = 6$); (2) data error $s = 0.01$ ($J = 6$); (3) first-scale regularization ($J = 5$); (4) second-scale regularization ($J = 4$).

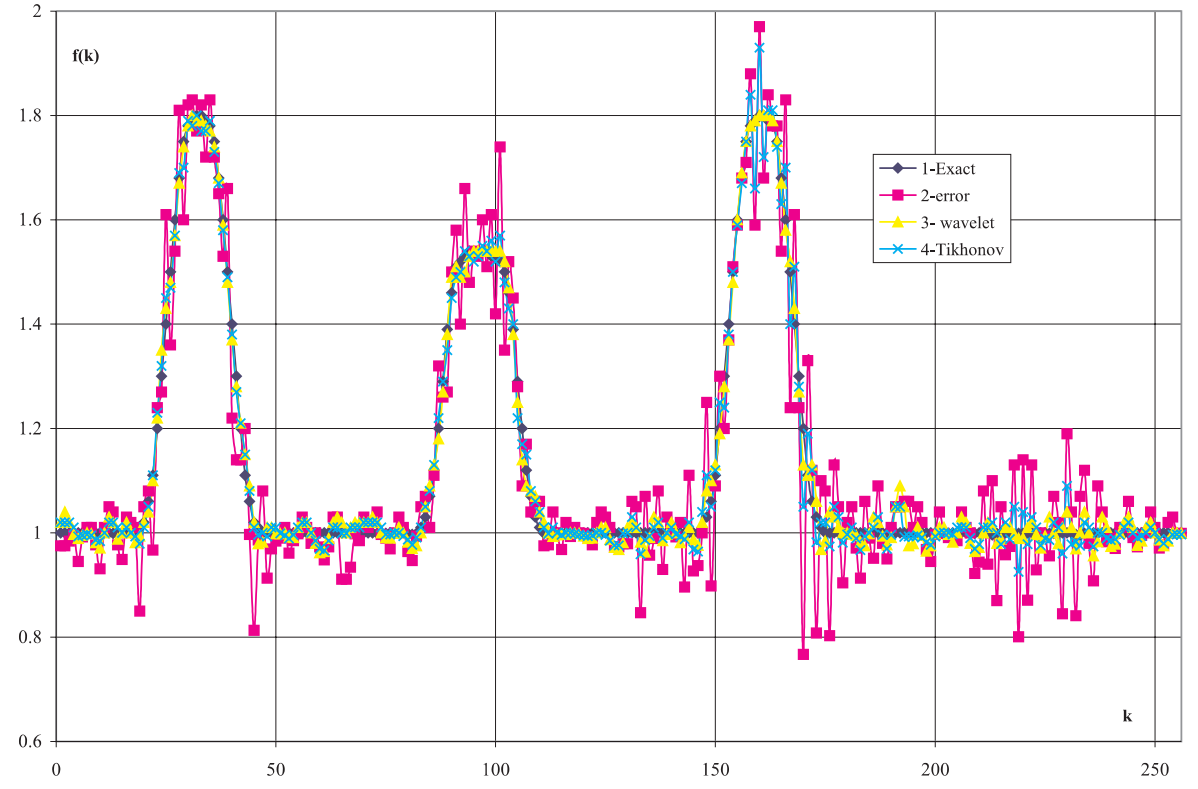

Fig. 4. Results of temperature estimation using different scales of wavelet transformation ($Re = 10\,000$): (1) exact inflow data ($J = 6$); (2) data error $\sigma = 0.01$ ($J = 6$); (3) first-scale regularization ($J = 5$); (4) second-scale regularization ($J = 4$).

Table 3

J	6	5	4	3
$\lambda_{\min}$	2.8×10^{-4}	1.9×10^{-3}	1.08×10^{-2}	5.5×10^{-2}

11. Comparison with Tikhonov regularization

In order to provide a comparison for the wavelet regularization, we consider the Tikhonov [9] regularization.

The standard Tikhonov regularization [4] of zero-order for the problem under consideration transforms the discrepancy (10) to

$$\varepsilon(f_\infty(Y)) = \int_Y (f^{\exp}(Y) - f(X_{\max}, Y))^2 \, \mathrm{d}Y + \alpha \int (f_\infty(Y))^2 \, \mathrm{d}Y,$$

where α is the regularization parameter. This variant of regularization provides unacceptable results (too smooth) for the inflow parameters. The addition of a second order regularization term $\alpha(f_{i+1} - 2f_i + f_{i-1})^2$ to the residual $\varepsilon(f)$ provides a much better quality (see Fig. 5). The result is similar in quality to the result obtained using the wavelet transformation (Fig. 3). Herein, we calculated the discrepancy for different α's and analyzed the variation of the discrepancy ε as a function of α and data error according to the discrepancy principle [4]. This search for the magnitude of a suitable regularization parameter α is not so transparent and does not provide an automatic procedure as the comparison of eigenvalue and data error used in wavelet regularization.

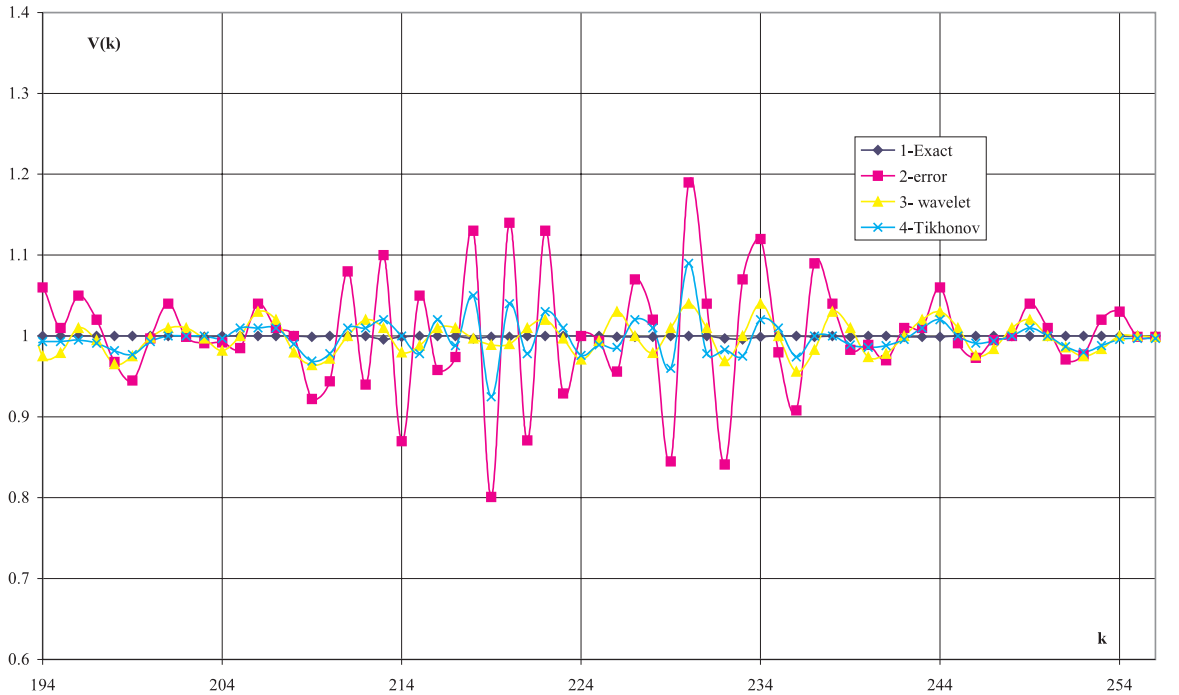

Fig. 5. The inflow parameter estimation from noisy ($\sigma = 0.01$) outflow parameters $f^{\exp}(Y)$ using second-order Tikhonov regularization (transversal velocity): (1) exact; (2) without regularization; (3) first-scale regularization ($J = 5$); (4) second-order Tikhonov regularization ($\alpha = 0.005$).

12. Conclusion

Numerical tests demonstrated a monotonous decreasing of the Hessian minimal eigenvalues as the scale of wavelet transformation decreases.

The new proposed algorithm is offered for control functions' space decomposition into "well-posed" and "ill-posed" subspaces for regularization of ill-posed problems.

This algorithm is based on multi-scale resolution (wavelet analysis) and Hessian minimal eigenvalue calculation using the solution of the second-order adjoint problem.

Numerical tests conducted with the two-dimensional parabolized Navier–Stokes equations demonstrated the applicability of this algorithm to the solution of the inverse-convection problem for optimally estimating inflow parameters from down-flow data.

This new approach can be readily extended to other problems where ill-posedness is present when adjoint parameter estimation is being carried out.

A comparison with the standard Tikhonov regularization of zeroth-order reveals that it yields unacceptable results for the inflow parameters, while a second-order Tikhonov regularization performs reasonably well, providing results comparable in quality to those obtained using the wavelet analysis. However, the choice of the regularization parameter for the Tikhonov second-order regularization is not transparent, i.e., one proceeds by trial and error – whereas the procedure in the newly proposed algorithm is automatic and efficient.

Appendix A. First-order adjoint problem

We now form the Lagrangian variation (11) with respect to $\Delta\rho, \Delta U, \Delta V, \Delta e$. By subtracting the undisturbed solution and retaining only first order terms we get

$$\begin{aligned}
\Delta\varepsilon_0(f_\infty(Y)) = \Delta\varepsilon(f_\infty(Y)) &+ \int_Y \int_X \left(U\frac{\partial(\Delta\rho)}{\partial X} + \rho\frac{\partial(\Delta U)}{\partial X} + \rho\frac{\partial(\Delta V)}{\partial Y} + V\frac{\partial(\Delta\rho)}{\partial Y} \right) \Psi_\rho \, \mathrm{d}X \, \mathrm{d}Y \\
&+ \int_Y \int_X \left(\Delta\rho\frac{\partial U}{\partial X} + \Delta U\frac{\partial\rho}{\partial X} + \Delta\rho\frac{\partial V}{\partial Y} + \Delta V\frac{\partial\rho}{\partial Y} \right) \Psi_\rho \, \mathrm{d}X \, \mathrm{d}Y \\
&+ \int_X \int_Y \left(U\frac{\partial\Delta U}{\partial X} + \Delta U\frac{\partial U}{\partial X} + \Delta V\frac{\partial U}{\partial Y} + V\frac{\partial\Delta U}{\partial Y} - \frac{1}{\rho Re}\frac{\partial^2\Delta U}{\partial Y^2} + \frac{\Delta\rho}{\rho^2 RE}\frac{\partial^2 U}{\partial Y^2} - \frac{\Delta\rho}{\rho^2}\frac{\partial P}{\partial X} \right. \\
&\left. + \frac{\kappa-1}{\rho}\left(\Delta\rho\frac{\partial e}{\partial X} + e\frac{\partial\Delta\rho}{\partial X} + \rho\frac{\partial\Delta e}{\partial X} + \Delta e\frac{\partial\rho}{\partial X} \right) \right) \Psi_U(X,Y) \, \mathrm{d}X \, \mathrm{d}Y \\
&+ \int_X \int_Y \left(U\frac{\partial\Delta V}{\partial X} + \Delta U\frac{\partial V}{\partial X} + \Delta V\frac{\partial V}{\partial Y} + V\frac{\partial\Delta V}{\partial Y} - \frac{4}{3\rho Re}\frac{\partial^2\Delta V}{\partial Y^2} + \frac{4\Delta\rho}{3\rho^2 Re}\frac{\partial^2 V}{\partial Y^2} - \frac{\Delta\rho}{\rho^2}\frac{\partial P}{\partial Y} \right. \\
&\left. + \frac{\kappa-1}{\rho}\left(\Delta\rho\frac{\partial e}{\partial Y} + e\frac{\partial\Delta\rho}{\partial Y} + \rho\frac{\partial\Delta e}{\partial Y} + \Delta e\frac{\partial\rho}{\partial Y} \right) \right) \Psi_V(X,Y) \, \mathrm{d}X \, \mathrm{d}Y \\
&+ \int_X \int_Y \left(U\frac{\partial\Delta e}{\partial X} + \Delta U\frac{\partial e}{\partial X} + \Delta V\frac{\partial e}{\partial Y} + V\frac{\partial\Delta e}{\partial Y} + (\kappa-1)\Delta e\left(\frac{\partial U}{\partial X} + \frac{\partial V}{\partial Y} \right) \right. \\
&+ (k-1)e\left(\frac{\partial\Delta U}{\partial X} + \frac{\partial\Delta V}{\partial Y} \right) \\
&\left. - \frac{1}{\rho Re}\left(\frac{\kappa}{Pr}\frac{\partial^2\Delta e}{\partial Y^2} - \frac{\kappa}{Pr}\frac{\Delta\rho}{\rho}\frac{\partial^2 e}{\partial Y^2} + \frac{8}{3}\left(\frac{\partial\Delta U}{\partial Y} \right)\left(\frac{\partial U}{\partial Y} \right) - \frac{\Delta\rho}{\rho}\frac{4}{3}\left(\frac{\partial U}{\partial Y} \right)^2 \right) \right) \Psi_e(X,Y) \, \mathrm{d}X \, \mathrm{d}Y.
\end{aligned} \tag{A.1}$$

After rearranging the terms with $\Delta\rho, \Delta U, \Delta V, \Delta e$ we obtain

$$\begin{aligned}
\Delta\varepsilon_0(f_\infty(Y)) = \int_X \int_Y \Bigg(& \left(U\frac{\partial(\Delta\rho)}{\partial X} + V\frac{\partial(\Delta\rho)}{\partial Y} \right) \Psi_\rho(X,Y) + \left(\frac{\partial U}{\partial X} + \frac{\partial V}{\partial Y} \right) \Psi_\rho \Delta\rho \\
& + \frac{\kappa-1}{\rho} \left(\frac{\partial(\Delta\rho)}{\partial Y} e + \Delta\rho \frac{\partial e}{\partial Y} \right) \Psi_V + \frac{\kappa-1}{\rho} \left(\frac{\partial(\Delta\rho)}{\partial X} e + \Delta\rho \frac{\partial e}{\partial X} \right) \Psi_U \\
& + \frac{\Delta\rho}{\rho^2} \left(-\frac{\partial P}{\partial X} + \frac{1}{Re} \frac{\partial^2 U}{\partial Y^2} \right) \Psi_U + \frac{\Delta\rho}{\rho^2} \left(-\frac{\partial P}{\partial Y} + \frac{4}{3Re} \frac{\partial^2 V}{\partial Y^2} \right) \Psi_V \\
& + \frac{\Delta\rho}{\rho^2} \left(\frac{\kappa}{Re\,Pr} \frac{\partial^2 e}{\partial Y^2} + \frac{4}{3Re} \left(\frac{\partial U}{\partial Y} \right)^2 \right) \Psi_e \Bigg) \, \mathrm{d}X \, \mathrm{d}Y \\
& + \int_X \int_Y \Bigg(\left(U\frac{\partial \Delta U}{\partial X} + \Delta U \frac{\partial U}{\partial X} + V\frac{\partial \Delta U}{\partial Y} - \frac{1}{\rho Re} \frac{\partial^2 \Delta U}{\partial Y^2} \right) \Psi_U(X,Y) + \frac{\partial \rho}{\partial X} \Psi_\rho \Delta U \\
& + \rho \frac{\partial \Delta U}{\partial X} \Psi_\rho + \Delta U \frac{\partial V}{\partial X} \Psi_V + \Delta U \frac{\partial e}{\partial X} \Psi_e + (\kappa-1) e \frac{\partial \Delta U}{\partial X} \Psi_e - \frac{8}{3Re} \frac{\partial U}{\partial Y} \frac{\partial \Delta U}{\partial Y} \Psi_e \Bigg) \, \mathrm{d}X \, \mathrm{d}Y \\
& + \int_X \int_Y \Bigg(\left(U\frac{\partial \Delta V}{\partial X} + \Delta V \frac{\partial V}{\partial Y} + V\frac{\partial \Delta V}{\partial Y} - \frac{4}{3\rho Re} \frac{\partial^2 \Delta V}{\partial Y^2} \right) \Psi_V(X,Y) + \Delta V \frac{\partial U}{\partial Y} \Psi_U \\
& + \rho \frac{\partial \Delta V}{\partial Y} \Psi_\rho + \Delta V \frac{\partial e}{\partial Y} \Psi_e + (\kappa-1) e \frac{\partial \Delta V}{\partial Y} \Psi_e \Bigg) \, \mathrm{d}X \, \mathrm{d}Y + \frac{\partial \rho}{\partial Y} \Psi_\rho \Delta V \\
& + \int_X \int_Y \Bigg(\left(U\frac{\partial \Delta e}{\partial X} + V\frac{\partial \Delta e}{\partial Y} + (\kappa-1)\Delta e \left(\frac{\partial U}{\partial X} + \frac{\partial V}{\partial Y} \right) - \frac{\kappa}{\rho Re\,Pr} \frac{\partial^2 \Delta e}{\partial Y^2} \right) \Psi_e(X,Y) \\
& + \frac{\kappa-1}{\rho} \left(\frac{\partial \rho}{\partial Y} \Delta e + \rho \frac{\partial \Delta e}{\partial Y} \right) \Psi_V + \frac{\kappa-1}{\rho} \left(\frac{\partial \rho}{\partial X} \Delta e + \rho \frac{\partial \Delta e}{\partial X} \right) \Psi_U \Bigg) \, \mathrm{d}X \, \mathrm{d}Y. \qquad \text{(A.2)}
\end{aligned}$$

We integrate this equation by parts and taking into account boundary conditions for $\Delta\rho, \Delta U, \Delta V, \Delta e$, respectively, we get

$$\Delta\varepsilon_0(f_\infty(Y)) =$$

Terms with $\Delta\rho$:

$$\begin{aligned}
& \int_Y \Psi_\rho U \Delta\rho \, \mathrm{d}Y \Big|_{X=0}^{X=1} - \int_Y \int_X \frac{\partial(U\Psi_\rho)}{\partial X} \Delta\rho \, \mathrm{d}X \, \mathrm{d}Y + \int_X \Psi_\rho V \Delta\rho \, \mathrm{d}X \Big|_{Y=0}^{Y=1} - \int_Y \int_X \frac{\partial(V\Psi_\rho)}{\partial Y} \Delta\rho \, \mathrm{d}X \, \mathrm{d}Y \\
& + \int_Y \int_X \left(\frac{\partial U}{\partial X} + \frac{\partial V}{\partial Y} \right) \Psi_\rho \Delta\rho \, \mathrm{d}X \, \mathrm{d}Y + (\kappa-1) \int_X \Psi_V e \rho^{-1} \Delta\rho \, \mathrm{d}X \Big|_{Y=0}^{Y=1} \\
& - (\kappa-1) \int_Y \int_X \frac{\partial(\Psi_V e/\rho)}{\partial Y} \Delta\rho \, \mathrm{d}X \, \mathrm{d}Y + (\kappa-1) \int_Y \Psi_U e/\rho \Delta\rho \, \mathrm{d}Y \Big|_{X=0}^{X=1} \\
& - (\kappa-1) \int_Y \int_X \frac{\partial(\Psi_U e/\rho)}{\partial X} \Delta\rho \, \mathrm{d}X \, \mathrm{d}Y + \int_Y \int_X \frac{\kappa-1}{\rho} \left(\frac{\partial e}{\partial Y} \Psi_V + \frac{\partial e}{\partial X} \Psi_U \right) \Delta\rho \, \mathrm{d}X \, \mathrm{d}Y \\
& + \int_Y \int_X \frac{1}{\rho^2} \Bigg(\left(-\frac{\partial P}{\partial X} + \frac{1}{Re} \frac{\partial^2 U}{\partial Y^2} \right) \Psi_U + \left(-\frac{\partial P}{\partial Y} + \frac{4}{3Re} \frac{\partial^2 V}{\partial Y^2} \right) \Psi_V \\
& + \left(\frac{\kappa}{Re\,Pr} \frac{\partial^2 e}{\partial Y^2} + \frac{4}{3Re} \left(\frac{\partial U}{\partial Y} \right)^2 \right) \Psi_e \Bigg) \Delta\rho \, \mathrm{d}X \, \mathrm{d}Y \\
& - \int_X \int_Y 2(\rho_{\mathrm{obs}}(X,Y) - \rho(X,Y)) \Delta\rho(X,Y) \delta(X - X_m) \delta(Y - Y_m) \, \mathrm{d}X \, \mathrm{d}Y +
\end{aligned}$$

terms with ΔU:

$$
\begin{aligned}
&+\int_Y \Psi_U U \Delta U \,\mathrm{d}Y\Big|_{X=0}^{X=1} - \int_Y \int_X \frac{\partial(U\Psi_U)}{\partial X}\Delta U \,\mathrm{d}X\,\mathrm{d}Y + \int_X \Psi_U V \Delta U \,\mathrm{d}X\Big|_{Y=0}^{Y=1}\\
&- \int_Y \int_X \frac{\partial(V\Psi_U)}{\partial Y}\Delta U \,\mathrm{d}X\,\mathrm{d}Y + \int_Y \Psi_\rho \rho \Delta U \,\mathrm{d}Y\Big|_{X=0}^{X=1} - \int_Y \int_X \frac{\partial(\Psi_\rho \rho)}{\partial X}\Delta U \,\mathrm{d}X\,\mathrm{d}Y\\
&+\int_Y \int_X \Psi_\rho \frac{\partial \rho}{\partial X}\Delta U \,\mathrm{d}X\,\mathrm{d}Y + \int_Y \int_X \left(+\frac{\partial U}{\partial X}\Psi_U + \frac{\partial V}{\partial X}\Psi_V + \frac{\partial e}{\partial X}\Psi_e\right)\Delta U \,\mathrm{d}X\,\mathrm{d}Y + \int_Y \Psi_e \frac{P}{\rho}\Delta U \,\mathrm{d}Y\Big|_{X=0}^{X=1}\\
&- \int_Y \int_X \frac{\partial}{\partial X}\left(\Psi_e \frac{P}{\rho}\right)\Delta U \,\mathrm{d}X\,\mathrm{d}Y - \frac{8}{3Re}\int_X \Psi_e \frac{\partial U}{\partial Y}\Delta U \,\mathrm{d}X\Big|_{Y=0}^{Y=1} + \frac{8}{3Re}\int_Y \int_X \frac{\partial}{\partial Y}\left(\Psi_e \frac{\partial u}{\partial Y}\right)\Delta U \,\mathrm{d}X\,\mathrm{d}Y\\
&- \int_X \frac{1}{\rho Re}\frac{\partial \Delta U}{\partial Y}\Psi_U \,\mathrm{d}X\Big|_{Y=0}^{Y=1} + \int_X \frac{\partial}{\partial y}\left(\frac{1}{\rho Re}\Psi_U\right)\Delta U \,\mathrm{d}Y\Big|_{Y=0}^{Y=1} - \int_Y \int_X \frac{\partial^2}{\partial y^2}\left(\frac{\mu}{\rho}\Psi_U\right)\Delta U \,\mathrm{d}X\,\mathrm{d}Y\\
&- \int_X \int_Y 2(U_{\mathrm{obs}}(X,Y) - U(X,Y))\Delta U(X,Y)\delta(X - X_m)\delta(Y - Y_m)\,\mathrm{d}X\,\mathrm{d}Y +
\end{aligned}
$$

terms with ΔV:

$$
\begin{aligned}
&+\int_Y \Psi_V U \Delta V \,\mathrm{d}Y\Big|_{X=0}^{X=1} - \int_Y \int_X \frac{\partial(U\Psi_V)}{\partial X}\Delta V \,\mathrm{d}X\,\mathrm{d}Y + \int_X \Psi_V V \Delta V \,\mathrm{d}X\Big|_{Y=0}^{Y=1} - \int_Y \int_X \frac{\partial(V\Psi_V)}{\partial Y}\Delta V \,\mathrm{d}X\,\mathrm{d}Y\\
&+\int_Y \int_X \left(\frac{\partial V}{\partial Y}\Psi_V + \frac{\partial U}{\partial Y}\Psi_U + \frac{\partial e}{\partial Y}\Psi_e\right)\Delta V \,\mathrm{d}X\,\mathrm{d}Y + \int_X \left(\Psi_\rho \rho + \frac{P}{\rho}\Psi_e\right)\Delta V \,\mathrm{d}X\Big|_{Y=0}^{Y=1}\\
&- \int_Y \int_X \frac{\partial}{\partial Y}\left(\Psi_\rho \rho + \frac{P}{\rho}\Psi_e\right)\Delta V \,\mathrm{d}X\,\mathrm{d}Y + \int_Y \int_X \Psi_\rho \frac{\partial \rho}{\partial Y}\Delta V \,\mathrm{d}X\,\mathrm{d}Y - \int_X \frac{4}{3\rho Re}\frac{\partial \Delta V}{\partial Y}\Psi_V \mathrm{d}X\Big|_{Y=0}^{Y=1}\\
&+\int_X \frac{\partial}{\partial y}\left(\frac{4}{3\rho Re}\Psi_V\right)\Delta V \,\mathrm{d}X\Big|_{Y=0}^{Y=1} - \frac{4}{3Re}\int_Y \int_X \frac{\partial^2}{\partial y^2}\left(\frac{1}{\rho}\Psi_V\right)\Delta V \,\mathrm{d}X\,\mathrm{d}Y - \int_X \int_Y 2(V_{\mathrm{obs}}(X,Y)\\
&- V(X,Y))\Delta V(X,Y)\delta(X - X_m)\delta(Y - Y_m)\,\mathrm{d}X\,\mathrm{d}Y +
\end{aligned}
$$

terms with Δe:

$$
\begin{aligned}
&\int_Y \Psi_e U \Delta e \,\mathrm{d}Y\Big|_{X=0}^{X=1} - \int_Y \int_X \frac{\partial(U\Psi_e)}{\partial X}\Delta e \,\mathrm{d}X\,\mathrm{d}Y + \int_X \Psi_e V \Delta e \,\mathrm{d}X\Big|_{Y=0}^{Y=1} - \int_Y \int_X \frac{\partial(V\Psi_e)}{\partial Y}\Delta e \,\mathrm{d}X\,\mathrm{d}Y\\
&+\int_Y \int_X \left(\frac{\kappa - 1}{\rho}\left(\frac{\partial \rho}{\partial Y}\Psi_V + \frac{\partial \rho}{\partial X}\Psi_U\right) + (\kappa - 1)\left(\frac{\partial U}{\partial X} + \frac{\partial V}{\partial Y}\right)\Psi_e\right)\Delta e \,\mathrm{d}X\,\mathrm{d}Y + (\kappa - 1)\int_X \Psi_V \Delta e \,\mathrm{d}X\Big|_{Y=0}^{Y=1}\\
&- (\kappa - 1)\int_Y \int_X \frac{\partial}{\partial Y}(\Psi_V)\Delta e \,\mathrm{d}X\,\mathrm{d}Y + (\kappa - 1)\int_Y \Psi_U \Delta e \,\mathrm{d}Y\Big|_{X=0}^{X=1} - (\kappa - 1)\int_Y \int_X \frac{\partial}{\partial X}(\Psi_U)\Delta e \,\mathrm{d}X\,\mathrm{d}Y\\
&- +\int_X \int_Y 2(e_{\mathrm{obs}}(X,Y) - e(X,Y))\Delta e(X,Y)\delta(X - X_m)\delta(Y - Y_m)\,\mathrm{d}X\,\mathrm{d}Y - \int_X \frac{\kappa}{\rho Re\, Pr}\frac{\partial \Delta e}{\partial Y}\Psi_e \,\mathrm{d}X\Big|_{Y=0}^{Y=1}\\
&+\int_X \frac{\partial}{\partial y}\left(\frac{\kappa}{\rho Re\, Pr}\Psi_e\right)\Delta e \,\mathrm{d}Y\Big|_{Y=0}^{Y=1} - \int_Y \int_X \frac{\partial^2}{\partial y^2}\left(\frac{\kappa}{\rho Re\, Pr}\Psi_e\right)\Delta e \,\mathrm{d}X\,\mathrm{d}Y. \qquad (A.3)
\end{aligned}
$$

We look for $(\Psi_\rho, \Psi_U, \Psi_V, \Psi_e)$ such that $\Delta\varepsilon_0 = \int_Y \mathrm{grad}(\varepsilon)\Delta f_\infty(Y)\,\mathrm{d}Y$ while all other first-order terms vanish. The corresponding conditions form the adjoint problem.

Acknowledgements

The second author acknowledges support from NSF grant ATM-97B1472 managed by Dr. Pamela Stephens.

References

[1] J. Liu, B. Gurrier, C. Denard, A sensitivity decomposition for regularized solution of inverse heart conduction problems by wavelets, Inverse Problems 11 (1995) 1177–1187.
[2] Z. Wang, I.M. Navon, F.X. LeDimet, X. Zou, The second order adjoint analysis: Theory and applications, Meteorol. Atmos. Phys. 50 (1992) 3–20.
[3] V.Yu. Terebigh, The restoration of images using minimal a priori information, Uspehi Fizicheskih Nauk, 165 (2) (1995) 143–176 (in Russian).
[4] O.M. Alifanov, E.A. Artyukhin, S.V. Rumyantsev, Extreme Methods for Solving Ill-Posed Problems with Applications to Inverse Heat Transfer Problems, Begell house Publishers, 1996.
[5] I. Daubechies, Orthonormal basis of compactly supported wavelets, Commun. Pure Appl. Math. 41 (7) (1988) 909–996.
[6] F.X. Le Dimet, O. Talagrand, Variational algorithms for analysis and assimilation of meteorological observations, Tellus 38A (2) (1986) 97–110.
[7] Liu, D.C. Jorge Nocedal, On the limited memory BFGS method for large scale minimization, Math. Prog. 45 (1989) 503–528.
[8] A.K. Alekseev, On estimation of spatial distribution of entrance boundary parameters from flowfield measurements for supersonic flow, Math. Model. 11 (12) (1999) 33–44.
[9] A.V. Tikhonov, V. Arsenin, Solution of Ill-posed Problems. Winston & Sons, Washington, DC, 1977, p. 224.
[10] Z. Wang, I.M. Navon, X. Zou, F.X. LeDimet, A truncated-Newton optimization algorithm in meteorology applications with analytic Hessian/vector products, Comput. Optimization Applications 4 (1995) 241–262.
[11] J. Liu, A sensitivity analysis for least-squares ill-posed problems using Haar basis, SIAM J. Numer. Anal. 31 (5) (1994) 1486–1496.